

# Integrating machine learning and deep learning with landscape metrics for urban heat island prediction

Siddharth Pal, Kavita Jhajharia

Department of Information Technology, Faculty of Science, Technology, and Architecture, Manipal University Jaipur, Jaipur, India

## Article Info

### Article history:

Received Jan 15, 2025

Revised Oct 6, 2025

Accepted Oct 18, 2025

### Keywords:

Deep learning

Long short-term memory

Machine learning

Socioeconomic data and

applications center

Urban heat island

## ABSTRACT

Elevated temperatures in urban areas relative to surrounding rural areas, known as the urban heat island (UHI) effect, constitute a pressing challenge to urban sustainability, public health, and energy efficiency. With a comprehensive global dataset from NASA's Socioeconomic Data and Applications Center (SEDAC) that encompasses land surface temperature (LST) and different urban characteristics, this study investigates the UHI phenomenon. The UHI intensity was predicted using advanced machine learning models, random forest, extreme gradient boosting (XGBoost), light gradient boosting machine (LightGBM), multilayer perceptron (MLP), and long short-term memory (LSTM) with attention mechanism. The LSTM with attention achieved top  $R^2$ : 0.9998 (day) and 0.9992 (night). Key landscape metrics include urban area size, population, and location. We analyzed spatial-temporal UHI patterns to identify local factors like geometry and vegetation. These findings are critical for urban planners and policy makers to identify targeted mitigation options, including green space expansion, the use of low thermal mass, and urban climate resilience strategies. These results advance predictive modeling, supporting resilient, and sustainable cities.

*This is an open access article under the [CC BY-SA](#) license.*



## Corresponding Author:

Kavita Jhajharia

Department of Information Technology, Faculty of Science, Technology, and Architecture

Manipal University Jaipur

Dehmi Kalan, Jaipur, Rajasthan, India

Email: kavita.jhajharia@jaipur.manipal.edu

## 1. INTRODUCTION

A natural phenomenon characterized by higher temperatures in urban areas and lower ones in rural surrounding areas is the urban heat island (UHI) effect caused by human and urban infrastructure activities. Proceeding factors like extensive use of heat retaining materials like asphalt and concrete, reduction in vegetative cover and anthropogenic heat generated by vehicles and industries [1] have caused this temperature disparity. Urbanization worsens UHI, increases cooling demand, pollution, and emissions [2]. UHI also raises health risks [3], harms biodiversity and strains infrastructure [4]. Given such impacts, UHI mitigation (e.g cool roofs and green spaces) is a priority [5], supported by better understanding of UHI dynamics. The research question in this study is as follows: do the landscape metrics (amplified by advanced machine learning (ML) and deep learning (DL) models) have the capacity to properly prophesy the intensity of UHI during both the day and night scenarios in various urban regions around the globe?

UHI impacts span environment, public health, and infrastructure, making them central to urban planning and climate readiness. Environmentally, UHI raises cooling demand, increasing emissions, and air pollution [2]. This feedback loop worsens UHI and accelerates climate change. UHI raises heat-related illnesses and deaths, especially in vulnerable groups [3]. Higher temperatures also increase vector-borne disease spread

[6]. UHI causes thermal stress on infrastructure, raising maintenance costs [7]. UHI also threatens biodiversity by forcing species to adapt to higher temperatures, leading to ecological imbalance [8]. Addressing these impacts is key for resilient, energy-efficient, sustainable cities.

Fundamentally, AI is changing how we study and mitigate UHI, plan cities, and adapt to climate change. ML models like convolutional neural networks (CNNs), random forest (RF), and support vector machine (SVM) analyze satellite and sensor data to pinpoint high-risk areas and assess temperature fluctuations [9], [10]. Using land surface temperature (LST) and local climate zones (LCZs) data, AI helps evaluate materials, density, and vegetation, guiding green infrastructure design [11]. One example is how applying genetic algorithms and particle swarm optimization (PSO) allows urban planners to estimate how well different interventions, i.e., the expansion of green spaces, growing vegetation, or use of reflective material, work in dense areas. They identify land use plans to reduce heat and boost resilience [12], [13]. Integrating remote sensing and AI enables tailored, data-driven UHI mitigation, supporting sustainable urban planning and public health. The importance lies in combining ML/DL models (including long short-term memory (LSTM) with attention) with large-scale global data (NASA Socioeconomic Data and Applications Center (SEDAC)). Including landscape metrics like urban size, population, and location reveals new spatial and temporal UHI trends. This work is unique since it is focused on a global scale, because of comparing the ML/DL models to predict the daytime and nighttime UHI, and providing recommendations which can be utilized by urban planners to restrict the heat island effects.

The identification of UHI is now transformative in addressing the increasing heat issues under the urban landscape considering the AI innovation in assessment and discernment. These tools use satellite, climate, and spatial data to track UHI precisely. CNNs analyze satellite images to map temperature gradients and produce urban heat maps [14]. Advanced deep neural networks (DNNs) and recurrent neural networks (RNNs) process temporal data to predict temperature trends, helping planners reduce heat effects [15]. Geographic information system (GIS) with AI creates layered heat maps showing where cooling measures like vegetation would be most effective [16]. ML in remote sensing analyzes unmanned aerial vehicle (UAV) and satellite thermal imagery for near real-time UHI monitoring [17]. Cloud computing scales AI to handle large data and support real-time urban planning. This keeps AI central to managing UHIs as cities grow and climate changes [18].

## 2. LITERATURE VIEW

Tehrani *et al.* [19] explores the use of the advanced ML models-e.g., gated recurrent units (GRU), DNN, and artificial neural networks (ANN) to learn to predict the UHI effect in European cities. It builds upon univariate datasets from 69 cities for 2007-2021 ( $n=0.56$  Gg), projecting to 2050, 2080 and using this and related datasets for the purpose of understanding the roles of urban morphology (spatial and structural features of urban landscapes) to UHI intensity. The study finds GRU highly accurate and shows denser urban forms increase UHI.

Yang *et al.* [20] addresses the critically important problem of the effect of the UHI on building energy use. UHI is a phenomenon whereby urbanized areas exhibit a temperature higher than surrounding rural areas, the heating of buildings increases energy demand, especially cooling over warmer months. It stresses accurate UHI assessment for sustainable development.

Assaf *et al.* [21] predict UHI severity using Bayesian networks applied to fine grained, census tract level data. This quantifies UHI impacts across varying density and vegetation. The study utilizes Bayesian networks to improve predictive accuracy by modeling the probabilistic relationships between these factors and thereby to provide a finer grained approach to the study of UHI patterns.

## 3. MATERIALS AND METHOD

The UHI effect, wherein urban areas have higher temperatures than surrounding rural regions, is investigated in this study. The major reason for this temperature disparity is primarily urban features including impervious surfaces such as paved roads and concrete structures, which absorb and retain heat. Additionally, excess heat is released from vehicles as well as heating and cooling systems [22].

### 3.1. Study area

This study used the global UHI datasets from 2013 from the NASA SEDAC [22] and included their LST measurements in degrees Celsius. Urban areas' average summer daytime maximums and nighttime minimums, along with the urban rural temperature difference are included in the dataset. Urban extents are defined as 10 km buffer zones around each area. The global rural-urban mapping project (GRUMPv1) is used to derive the urban boundaries while the temperature data are derived from parts of the moderate resolution imaging spectroradiometer (MODIS) on NASA's Aqua satellite. This dataset is geographically wide covering multiple continents from varying portions of North and South America, Africa, Asia, Europe, and Oceania.

This swath extends from latitude 78.28°N to -54.86°S, and longitude 179.46°E to -176.2°W, providing a global example of the UHI effect. Temperature data were recorded over 40-day period during the peak of summer months from July to August in the northern hemisphere, and from January to February in the southern hemisphere.

### 3.2. Data collection and pre-processing

#### 3.2.1. Data collection

For this study, the data used in it comes from the global UHI dataset, 2013 from NASA SEDAC, Center for International Earth Science Information Network (CIESIN), Columbia University [22]. The LST values are available as this dataset, which are land LST values for urban and rural areas derived from MODIS satellite data. During peak summer months the dataset contains temperature readings for daytime maximum as well as nighttime minimum temperatures. As a preview, Table 1 presents some of the sample entries in the dataset. This assists to explain the nature of demographic and geographic information enclosed in the analysis. The data set used in this study also includes urban area codes, names, and estimated populations, which form the basis for sample population estimates.

Table 1. A preview of dataset used in research work

ISOURLID	ISO3	URBID	NAME	SCHNM	ES90POP	ES95POP	ES00POP
GRL8	GRL	8	Upernavik	UPERNAVIK	918	1015	1123
USA15	USA	15	Barrow	BARROW	3469	3986	4581
NOR17	NOR	17	Honningsvåg	HONNINGSVAG	2237	2356	2510
NOR19	NOR	19	Havøysund	HAVOYSUND	1285	1235	1163
NOR21	NOR	21	Kjøllefjord	KJOLLEFJORD	1159	1115	1049
NOR26	NOR	26	Berlevåg	BERLEVAG	1297	1247	1174
GRL31	GRL	31	Uummannaq	UUMMANNAQ	1405	1422	1440
RUS40	RUS	40	Anadyr	ANADYR	12054	12035	11900
WLF52	WLF	52	Mata'utu	MATAUTU	1222	1150	1083

#### 3.2.2. Data pre-processing

We preprocessed the dataset for modeling. In the presence of high cloud cover, missing temperature values were filled with alternative period data (April to May 2013 for the northern hemisphere, and December 2013 to January 2014 for the southern hemisphere) [22]. We excluded regions without UHI or urban areas. We mapped and aggregated urban-rural temperatures. Seasonal data were aligned across hemispheres. Normalization reduced geographic/climatic bias.

#### 3.2.3. Workflow

The primary task of this work is to predict the UHI effect, i.e. the temperature difference between the urban and surrounding rural area ( $D\_T\_DIFF$ ) and at night ( $N\_T\_DIFF$ ). We use a dataset including urban and buffer area temperature observations, urban area size, population estimates, geographical coordinates, to achieve this. The temperature differences are predicted using a collection of multiple ML models consisting of RF-regressor, extreme gradient boosting (XGBoost)-regressor, light gradient boosting machine (LightGBM), multilayer perceptron (MLP), and LSTM with attention mechanism on these features. Finally, we evaluate the performance of the model using different error metrics such as root mean squared error (RMSE), mean squared error (MSE), mean absolute error (MAE), and coefficient of determination ( $R^2$ ) (to ensure good predictions of the UHI effect across the other regions). Figure 1 represents the flowchart of the research.

#### 3.2.4. Landscape metrics

Landscape metrics in urban studies and environmental science are important to quantify spatial patterns in landscape features for describing underlying environmental phenomena such as the UHI effect. In predicting UHI, landscape metrics quantify these characteristics of the urban area and surrounding land: including land use types, land cover, and spatial configuration directly influencing the thermal properties of the study area. Several landscape metrics are used to characterize the studied urban areas and their associated 10 km buffer zones. These metrics include:

- Urban area size (SQKM\_FINAL): a comparison was made of the extent in square kilometres that defines 'urban' and the impact it has on the local temperature variation. Impervious surfaces in larger urban areas cover more surface area that results in a more significant UHI effect [1].
- Population estimates (ES95POP): since a significant contributor to waste heat in urban areas is the level of human activity, the estimated population of urban areas in 1995 is used as proxy for it. The UHI effect

is often associated with higher population densities with corresponding heightened energy consumption and heat production [7].

- Temperature variability (URB\_D\_MEAN, BUF\_D\_MEAN, URB\_N\_MEAN, BUF\_N\_MEAN): the urban and its buffer are defined by a buffer area surrounding the urban area at a scale of 1:10,000, and these metrics represent the average daytime maximum and average nighttime minimum LSTs for urban area and its buffer. Direct indicators of the UHI effect and the meaning of the thermal land scape performance are D\_T\_DIFF (day) and N\_T\_DIFF (night), the temperature differences between urban and rural areas [22].
- Geographic location (LATITUDE, LONGITUDE): geographic location of the urban areas is corresponded to the climatic condition of the region because temperature variation is dependent on the latitude, altitude, and nearness to mountains or bodies of water. Locally, these geographic characteristics play a major role in local differences in temperature between urban and rural areas [23].
- Land cover and impervious surface area: while not explicitly a part of this dataset, the percentage of paved roads, buildings, etc. and land cover types (for example green space, water body) of an area also plays a major role in the UHI effect. These variables can be derivable from satellite imagery or other spatial datasets and crucial for understanding the reasons for differences in temperatures between the urban and rural zones [24], [25].

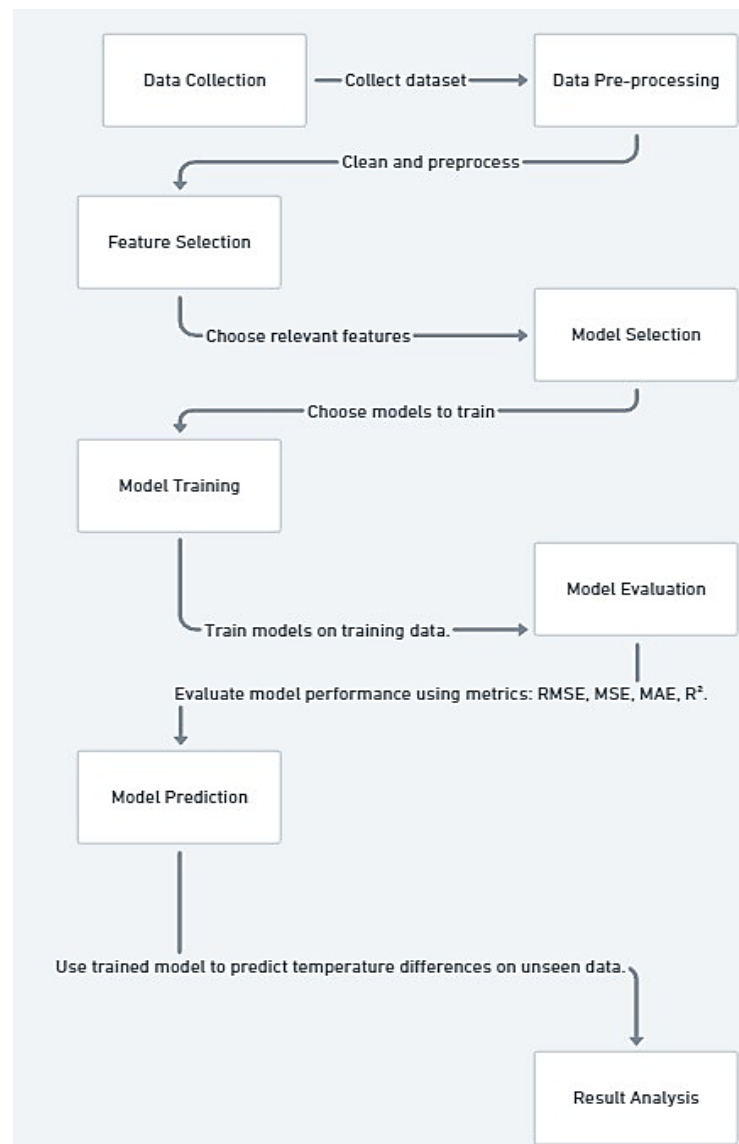


Figure 1. Demonstrating workflow of research work

#### 4. RESULT AND DISCUSSION

UHI has been analyzed vis urban-rural temperature differences and compared ML models. Our goal is to find UHI patterns and predictive models for urban planning. For the evaluation, we adopted key scores, namely  $R^2$ , RMSE, MAE, and MSE to measure the proportion of variance predicted by the model, mean magnitude of errors, mean absolute difference of predicted and actual values and the MSE of prediction respectively.

##### 4.1. Exploratory data analysis

Exploratory data analysis (EDA) has been performed to identify patterns important for predicting UHI. We analyzed distributions of numeric variables as shown in Figure 2. Some features were skewed, others normal; thus feature scaling was applied. Figure 3 shows feature scatter plots and relationships. We wanted to know whether there is difference between clustered areas and buffer areas for some feature pairs; and for some, urban regions have different degree of clusters compared to buffer areas, meaning that urbanization has an effect on some of the feature pairs. Detected correlations, like between temperature and built-up density, align with UHI trends.

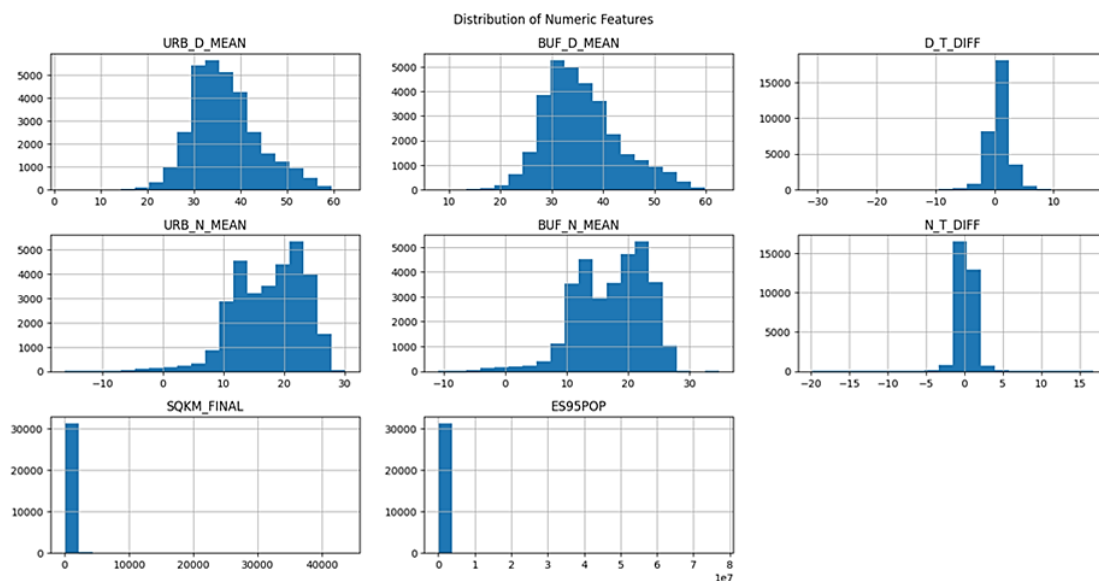


Figure 2. The plot shows distribution of numeric attributes throughout the dataset

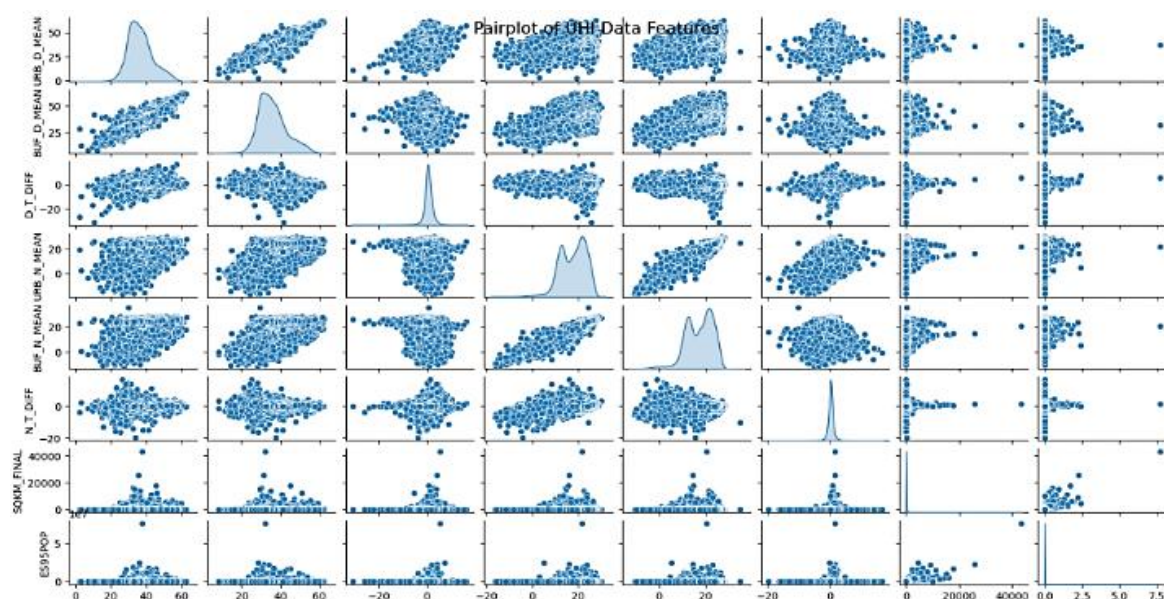


Figure 3. Pairwise relationships of data features (Pairplot)

#### 4.2. Model performance comparison

The evaluation of ML models for UHI prediction using RMSE, MSE, and MAE has been done. We analysed the performance of five models: RF-regressor, XGBoost-regressor, LightGBM, MLP, and LSTM with an attention mechanism. The LSTM with attention was the best performing model and is presented as following the lowest RMSE, equal to 0.0253 (day), 0.0314 (night) and MAE, equal to 0.0079 (day), 0.0113 (night), and the highest  $R^2$  values, equal to 0.9998 (day), 0.9992 (night). The MLP also showed good results with  $R^2=0.9973$  (day) and 0.9975 (night) and RMSE=0.0986 (day), 0.0557 (night). RF and LightGBM brought excellent results, and RF got the highest  $R^2$  values of 0.9917 (day) and 0.9683 (night) with the lowest RMSE of 0.1726 and 0.1986 LightGBM achieved  $R^2$  values 0.9736 (day) and 0.9302 (night) and RMSE of 0.3081 and 0.2948. Closely behind was the XGBoost, which had slightly worse accuracy of  $R^2$  equal to 0.9731 (day) and 0.9638 (night) and RMSE equal to 0.3109 and 0.2122 respectively. The Figure 4 represents the comparison of all models. Figure 5 represents the comparison of the scatter plot of the models. Figure 5 shows actual vs. predicted values scatter plots of each model: Figure 5(a) RF is moderately accurate; Figure 5(b) XGBoost also performs similarly with the performance having a touch more dispersion; Figure 5(c) LightGBM is more scattered and has a lower  $R^2$ ; Figure 5(d) MLP has a high classification accuracy; and Figure 5(e) LSTM with attention presents the fitting points at a close distance to the diagonal. These plots describe the predictive performance of each of these models.

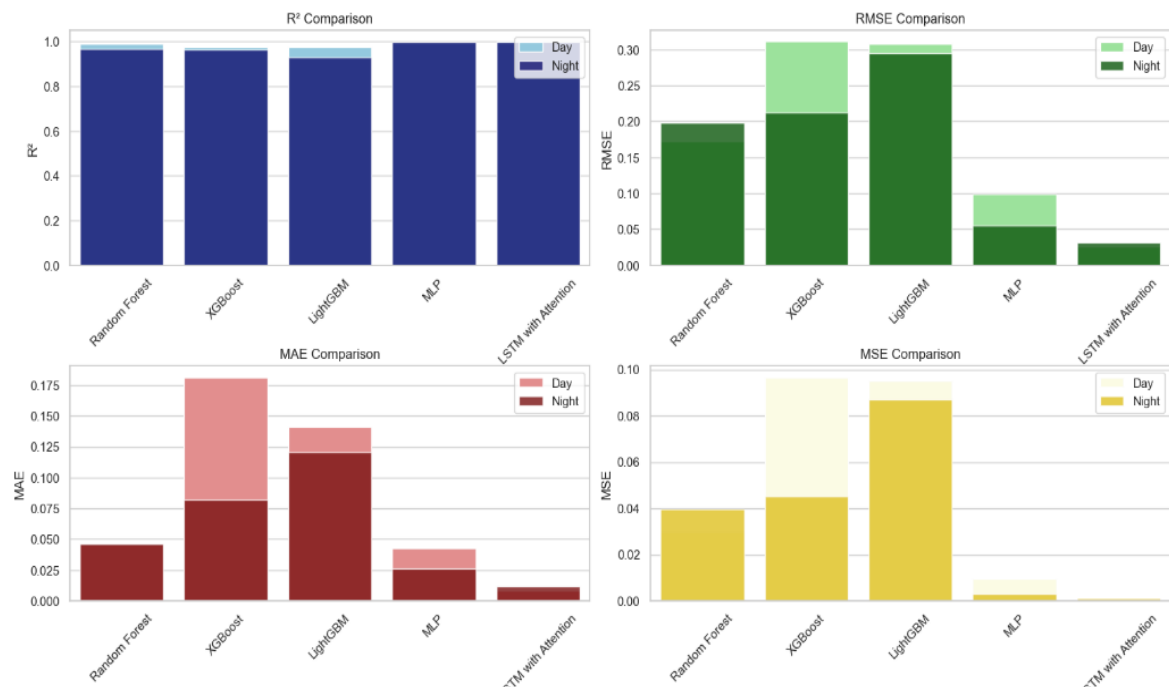


Figure 4. A bar chart of the metrics performed across the day and night dataset for both the models and performs a comparative analysis of the models' performances

#### 4.3. Day vs. night performance

Models performed better during the daytime with lower errors. Daytime data are more stable and predictable. However, prediction errors were higher for nighttime data that may be related to greater variability in nighttime cooling rates, microclimatic influences, or some other such factors affecting heat retention, such as urban geometry or the distribution of vegetation. Figure 6 represents the temperature difference between day and night. Both show scatter around zero, with greater spread and sensitivity to outliers at night.

The daytime temperatures differences in the kernel density estimation (KDE) plot (blue curve) shows a wider distribution of errors with a maximum around zero, indicating good prediction but with greater variability as shown in Figure 7. This wider distribution is indicative of poorer performance with daytime conditions, which may be explained by a stronger dependence on atmospheric dynamics from solar radiation or localized weather events, for instance. The tails show some instances of large over tensions or under tensions that warrant further study to identify reasons.



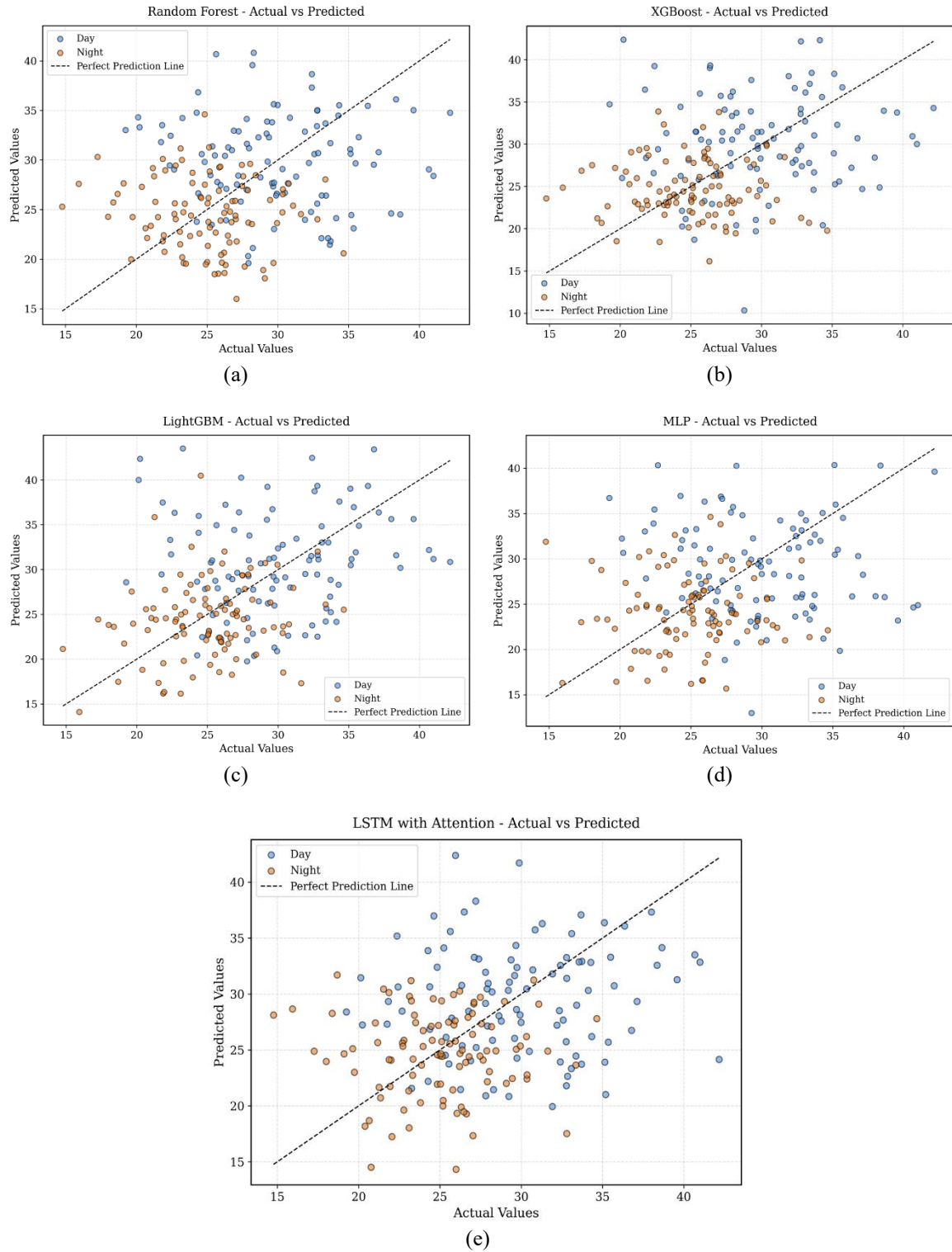


Figure 5. The representation of actual vs. predicted plot for (a) RF, (b) XGBoost, (c) LightGBM, (d) MLP, and (e) LSTM

While nighttime temperature differences (red curve) reveal a much sharper and narrower peaked profile centered around zero, indicating much more consistent and reliable prediction during the night. This demonstrates that the model performs better in stable nighttime conditions, where there are few environmental fluctuations. This narrow spread and short tails suggest the model is robust for nighttime temperature patterns.

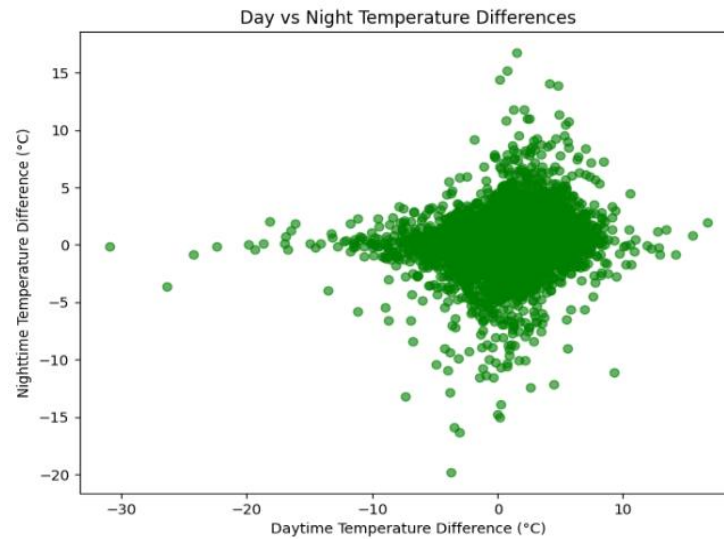


Figure 6. The scatter plot shows day vs night temperature differences

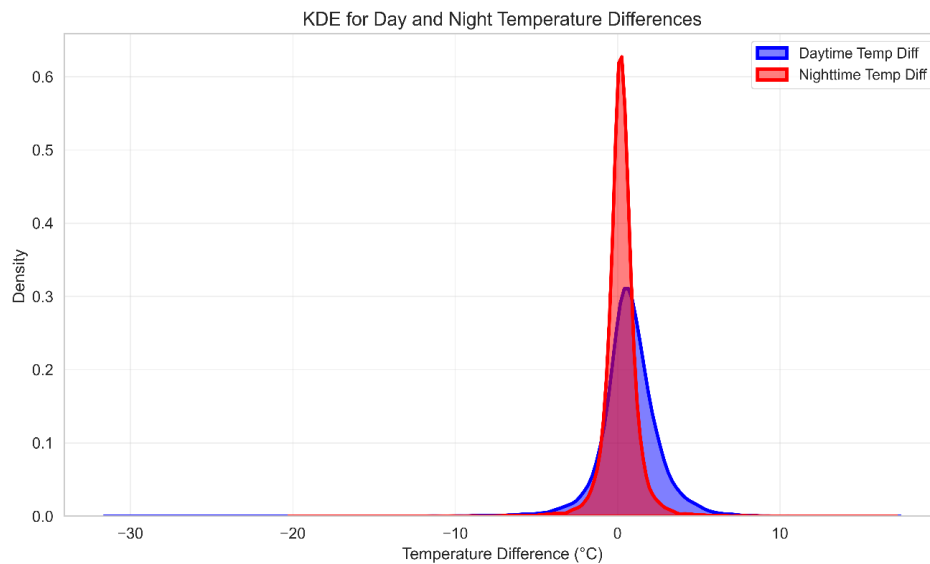


Figure 7. Kernel density estimate at day and night temperature differences

## 5. CONCLUSION

For predicting UHI effects, different ML models were tested in this study using day and night temperature data. The best performing model was an LSTM with attention mechanism among the models tested. It achieved the lowest error metrics (RMSE, MSE, and MAE) and the highest  $R^2$  scores for both day ( $R^2=0.9998$ ) and night ( $R^2=0.9992$ ). Its unique ability to extract some of the data's complex temporal patterns and dependencies makes it a powerful tool for UHI prediction, especially as it tackles spatial and temporal variation. We analyzed spatial and temporal UHI trends. However, daytime predictions exhibited greater variability across models relative to nighttime predictions, which highlights the day-to-day nature of daytime conditions affected by factors such as solar radiation, urban geometry, and vegetation cover. Nighttime stability improved model consistency. Spatial analysis shows sprawl variation, suggesting local solutions. LSTM helps planners target high-risk areas with fine-grained predictions. There are multiple practical implications of the study: urban planners will be able to locate high-risk areas and plan special provisions, including the enlargement of green spaces and the utilisation of reflective materials. Limitations include reliance on satellite LST, which may miss local microclimates. Further work could use real-time sensor data, higher resolution imagery, and socio-economic factors to improve accuracy and guide local UHI mitigation.



FUNDING INFORMATION

Authors state no funding involved.

AUTHOR CONTRIBUTIONS STATEMENT

This journal uses the Contributor Roles Taxonomy (CRediT) to recognize individual author contributions, reduce authorship disputes, and facilitate collaboration.

Name of Author	C	M	So	Va	Fo	I	R	D	O	E	Vi	Su	P	Fu
Siddharth Pal	✓	✓		✓	✓	✓		✓	✓		✓			
Kavita Jhahharia	✓			✓			✓			✓		✓		

C : Conceptualization	I : Investigation	Vi : Visualization
M : Methodology	R : Resources	Su : Supervision
So : Software	D : Data Curation	P : Project administration
Va : Validation	O : Writing - Original Draft	Fu : Funding acquisition
Fo : Formal analysis	E : Writing - Review & Editing	

CONFLICT OF INTEREST STATEMENT

Authors state no conflict of interest.

DATA AVAILABILITY

The authors confirm that the data supporting the findings of this study are available within the article.

REFERENCES

[1] J. Kong, Y. Zhao, D. Strebel, K. Gao, J. Carmeliet, and C. Lei, "Understanding the impact of heatwave on urban heat in greater sydney: temporal surface energy budget change with land types," *Science of The Total Environment*, vol. 903, Dec. 2023, doi: 10.1016/j.scitotenv.2023.166374.

[2] T. P. Scolaro, E. Ghisi, and C. M. Silva, "Effectiveness of cool and green roofs inside and outside buildings in the brazilian context," *Sustainability*, vol. 16, no. 18, Sep. 2024, doi: 10.3390/su16188104.

[3] S. Chauhan, C. L. Walsh, P. Eckersley, E. Mohareb, and O. Heidrich, "Urban heat stress, air quality and climate change adaptation strategies in UK cities," *Frontiers of Engineering Management*, vol. 12, no. 2, pp. 255–271, Jun. 2025, doi: 10.1007/s42524-025-4029-y.

[4] S. Chen *et al.*, "Impact of urbanization on the thermal environment of the chengdu–chongqing urban agglomeration under complex terrain," *Earth System Dynamics*, vol. 13, no. 1, pp. 341–356, Feb. 2022, doi: 10.5194/esd-13-341-2022.

[5] J. Canton and A. Dipankar, "Climatological analysis of urban heat island effects in Swiss cities," *International Journal of Climatology*, vol. 44, no. 5, pp. 1549–1565, Apr. 2024, doi: 10.1002/joc.8398.

[6] M. D. Castillo *et al.*, "Quantifying the health benefits of urban climate mitigation actions: current state of the epidemiological evidence and application in health impact assessments," *Frontiers in Sustainable Cities*, vol. 3, Nov. 2021, doi: 10.3389/frsc.2021.768227.

[7] E. D. Cristo, L. Evangelisti, L. Barbaro, R. D. L. Vollaro, and F. Asdrubali, "A systematic review of green roofs' thermal and energy performance in the mediterranean region," *Energies*, vol. 18, no. 10, May 2025, doi: 10.3390/en18102517.

[8] K. Joshi, A. Khan, P. Anand, and J. Sen, "Understanding the synergy between heat waves and the built environment: a three-decade systematic review informing policies for mitigating urban heat island in cities," *Sustainable Earth Reviews*, vol. 7, no. 1, Aug. 2024, doi: 10.1186/s42055-024-00094-7.

[9] S. Liu, J. Zhang, J. Li, Y. Li, J. Zhang, and X. Wu, "Simulating and mitigating extreme urban heat island effects in a factory area based on machine learning," *Building and Environment*, vol. 202, Sep. 2021, doi: 10.1016/j.buildenv.2021.108051.

[10] B. Sirmacek and R. Vinuesa, "Remote sensing and ai for building climate adaptation applications," *Results in Engineering*, vol. 15, Sep. 2022, doi: 10.1016/j.rineng.2022.100524.

[11] O. Y. A. Mohamed and I. Zahidi, "Artificial intelligence for predicting urban heat island effect and optimising land use/land cover for mitigation: prospects and recent advancements," *Urban Climate*, vol. 55, May 2024, doi: 10.1016/j.uclim.2024.101976.

[12] A. Shaamala, T. Yigitcanlar, A. Nili, and D. Nyandega, "Algorithmic green infrastructure optimisation: review of artificial intelligence driven approaches for tackling climate change," *Sustainable Cities and Society*, vol. 101, Feb. 2024, doi: 10.1016/j.scs.2024.105182.

[13] M. D. Sala, M. Hendrick, and G. Manoli, "Universal scaling of intra-urban climate fluctuations," *arXiv:2505.19998*, May 2025.

[14] M. Z. U. Rehman, S. M. S. Islam, D. Blake, A. Ulhaq, and N. Janjua, "Deep learning for land use classification: a systematic review of HS-LiDAR imagery," *Artificial Intelligence Review*, vol. 58, no. 9, Jun. 2025, doi: 10.1007/s10462-025-11265-z.

[15] G. Tanoori, A. Soltani, and A. Modiri, "Machine learning for urban heat island (UHI) analysis: predicting land surface temperature (LST) in urban environments," *Urban Climate*, vol. 55, 2024, doi: 10.1016/j.uclim.2024.101962.




[16] G. Mutani, A. Scalise, X. Sufa, and S. Grasso, "Synergising machine learning and remote sensing for urban heat island dynamics: a comprehensive modelling approach," *Atmosphere*, vol. 15, no. 12, Nov. 2024, doi: 10.3390/atmos15121435.

[17] C. R. de Almeida, A. C. Teodoro, and A. Gonçalves, "Study of the urban heat island (UHI) using remote sensing data/techniques: a systematic review," *Environments*, vol. 8, no. 10, Oct. 2021, doi: 10.3390/environments8100105.




- [18] H. Shi, G. Xian, R. Auch, K. Gallo, and Q. Zhou, "Urban heat island and its regional impacts using remotely sensed thermal data—a review of recent developments and methodology," *Land*, vol. 10, no. 8, Aug. 2021, doi: 10.3390/land10080867.
- [19] A. A. Tehrani *et al.*, "Predicting urban heat island in European cities: a comparative study of GRU, DNN, and ANN models using urban morphological variables," *Urban Climate*, vol. 56, Jul. 2024, doi: 10.1016/j.uclim.2024.102061.
- [20] M. Yang, H. Wang, C. W. Yu, and S.-J. Cao, "A global challenge of accurately predicting building energy consumption under urban heat island effect," *Indoor and Built Environment*, vol. 32, no. 3, pp. 455–459, Mar. 2023, doi: 10.1177/1420326X221123222.
- [21] G. Assaf, X. Hu, and R. H. Assaad, "Predicting urban heat island severity on the census-tract level using bayesian networks," *Sustainable Cities and Society*, vol. 97, Oct. 2023, doi: 10.1016/j.scs.2023.104756.
- [22] NASA, "Global urban heat island (UHI) data set, 2013," *Earth Science Data Information System*. 2013. Accessed: Nov. 15, 2024. [Online]. Available: <https://www.earthdata.nasa.gov/data/catalog/sedac-ciesin-sedac-sdei-uhi2013-1.0>
- [23] B. Zhou, D. Rybski, and J. P. Kropp, "The role of city size and urban form in the surface urban heat island," *Scientific Reports*, vol. 7, no. 1, Jul. 2017, doi: 10.1038/s41598-017-04242-2.
- [24] S. Cheval *et al.*, "A systematic review of urban heat island and heat waves research (1991–2022)," *Climate Risk Management*, vol. 44, 2024, doi: 10.1016/j.crm.2024.100603.
- [25] L. Zhao, X. Fan, and T. Hong, "Urban heat island effect: remote sensing monitoring and assessment—methods, applications, and future directions," *Atmosphere*, vol. 16, no. 7, Jun. 2025, doi: 10.3390/atmos16070791.

## BIOGRAPHIES OF AUTHORS



**Siddharth Pal**    is an undergraduate student pursuing a B.Tech. in Information Technology at Manipal University Jaipur. His research interests include machine learning, federated learning, and computer vision, with a growing focus on large language models and knowledge graphs. He is currently a technical intern (research) at Siemens Technology, Bangalore, in their central Department of R&D (FT RPD), where he is working on projects involving LLMs and knowledge graph applications. In parallel, he is also a research intern at IIT BHU, contributing to a DRDO-funded project on scalable federated learning frameworks for resource-constrained edge devices. Previously, he completed a research internship at NIT Mizoram. He can be contacted at email: [siddharth.229302284@mun.manipal.edu](mailto:siddharth.229302284@mun.manipal.edu).



**Kavita Jhahharia**    has received her B.Tech. degree from Rajasthan Technical University, India, in 2013 in Information Technology, and the M.Tech. degree from SRM University, Sonapat, India, in 2016. She has completed her Ph.D. degree from Manipal University Jaipur. She is Assistant Professor in Manipal University Jaipur since 2016. She is member of ACM. Her research interest is artificial intelligence, wireless networking, and software engineering. She can be contacted at email: [kavita.chaudhary@outlook.com](mailto:kavita.chaudhary@outlook.com).